This is the post-print version of the article published in ACS Med. Chem. Lett, 2019 Apr 11; 10(4): 469-474

Discovery of the First-in-Class GSK-3β/HDAC Dual Inhibitor as Disease-Modifying Agent To Combat Alzheimer's Disease

Angela De Simone,[†◆] Valeria La Pietra,[‡◆] Nibal Betari,[†] Nicola Petragnani,[§] Mariarosaria Conte,[∥] Simona Daniele,[⊥] Deborah Pietrobono,[⊥] Claudia Martini,[⊥] Sabrina Petralla,[#] Raffaella Casadei,[†] Lara Davani,[†] Flavia Frabetti,[▽] Pasquale Russomanno,[‡] Ettore Novellino,[‡] Serena Montanari,[†] Vincenzo Tumiatti,[†] Patrizia Ballerini,[§] Federica Sarno,[○] Angela Nebbioso,[○] Lucia Altucci,[○] Barbara Monti,[#] Vincenza Andrisano,[†] and Andrea Milelli[*†]

Abstract

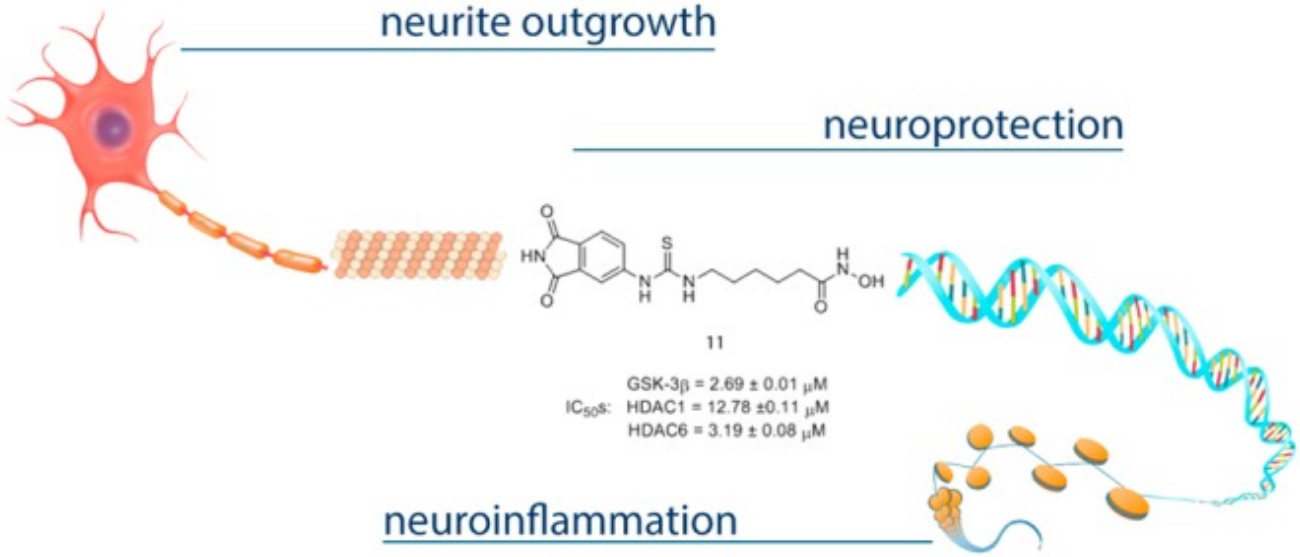

Several evidence pointed out the role of epigenetics in Alzheimer's disease (AD) revealing strictly relationships between epigenetic and "classical" AD targets. Based on the reported connection among histone deacetylases (HDACs) and glycogen synthase kinase 3β (GSK-3β), herein we present the discovery and the biochemical characterization of the first-in-class hit compound able to exert promising anti-AD effects by modulating the targeted proteins in the low micromolar range of concentration. Compound **11** induces an increase in histone acetylation and a reduction of tau phosphorylation. It is nontoxic and protective against H_2O_2 and 6-OHDA stimuli in SH-SY5Y and in CGN cell lines, respectively. Moreover, it promotes neurogenesis and displays immunomodulatory effects. Compound **11** shows no lethality in a wt-zebrafish model (<100 μM) and high water solubility.

Keywords: Polypharmacology, epigenetics, dual binding agents, glycogen synthase kinase 3β, histone deacetylases, neuroprotection

Alzheimer's disease (AD) represents the most common cause of dementia, and it is a pathological condition for which a cure is not available. Unfortunately, it is also the disease with the highest attrition rates in drug discovery (99.6% of failure rate). Indeed, since Memantine's approval, no candidates have successfully completed the clinical trials and no new drugs are on the horizon.[1] In this context, it is not surprising the decision of some big companies to end R&D on new anti-AD drugs.[2] The failures of intense decades of research from both industry and academia may be due to the incomplete knowledge of the physiopathological events that lead to the onset of the pathology.[3] Due to the complexity of AD, it is now widely accepted that it could be better contrasted by a chemical entity able to simultaneously modulate multiple targets involved in the onset of the disease. It is an accepted belief that a single compound able to fulfill such a task should more significantly impact the course of disease progression.[4] However, the development of multitarget ligands is a huge challenge in terms of target selection, molecules design, and physical–chemical properties requirements of the designed molecules.[5] Plenty of ligands have been developed so far hitting a single or multiple targets acting on different and not strictly related pathways believed important in AD pathogenesis, such as acetylcholinesterase, monoamino oxidases, oxidative stress, metal dyshomeostasis, etc.[6,7] Besides the aforementioned classical and deeply explored targets, some other proteins have been recognized as validated target for AD, like glycogen synthase kinase (GSK-3β), considered one of the most attractive due to its pivotal role in this disorder.[8] It is a key signaling enzyme in AD especially known for its capacity to modulate tau hypherphosphorylation. However, since the epigenetic modification is considered a new promising frontier for the study and treatment of AD,[9] the interest in regulating histone acetylation through histone deacetylases (HDACs) is rising up. The emerging role of HDACs as AD target is also supported by the evidence of the role of histone acetylation in rescuing learning and memory impairment.[10] Several connections between GSK-3β and HDACs have been highlighted. D'Mello and co-workers have shown that the neurotoxic effects of HDAC1 depend on GSK-3β activity, and in turn, the pharmacological blockage of such activity prevents HDAC1-induced neuronal death in cerebellar granule neurons (CGNs).[11] In hippocampal neurons, GSK-3β and HDAC6 were found in the same protein complex in which GSK-3β phosphorylates HDAC6 enhancing its activity.[12] It is worth noting that elevated HDAC6 activity increases tau phosphorylation interfering with its propensity to aggregate and the HDAC6-selective inhibitor tubacin attenuates tau phosphorylation.[13] Furthermore, both GSK-3β and class I–II HDAC inhibitors are able to shift microglia from the neurotoxic activation (M1, proinflammatory) to the neuroprotective (M2, antiinflammatory) phenotype.[14] Moreover, it is reported that combined inhibition of GSK-3β and HDACs induces synergistic neuroprotective effects compared to the single drug with a potential improved therapeutic selectivity.[15–17] Based on the above considerations, herein we report the design, synthesis, and preliminary biological evaluations of the first class of dual GSK-3β/HDACs inhibitors (Figure1). Specifically, compound **11** shows the best biochemical profile opening up the road for the development of new groundbreaking anti-AD agents.

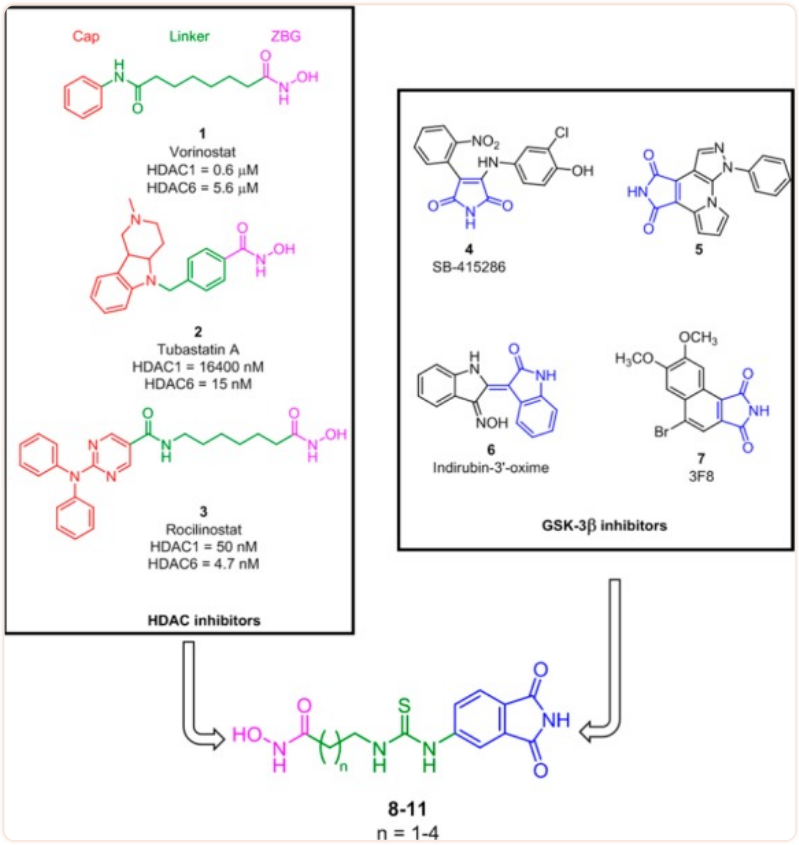

Figure 1

Drug design strategy leading to compounds **8**–**11**. On the top-left, the pharmacophore features of known HDACs inhibitors are highlighted: a cap group, a linker, and a zinc-binding group (ZBG) (colored in red, green, and magenta, respectively). On the top-right, some GSK-3β inhibitors containing the phthalimide-like function (depicted in blue).

Results and Discussion

Design

In order to design dual HDACs/GSK-3β inhibitors, we sought to combine in a single chemical entity the pharmacophoric groups responsible for binding to GSK-3β and HDACs (Figure1). Looking at known HDAC inhibitors (i.e., **1**–**3** in Figure1),[18–20] it emerges that the following pharmacophore features are present: the hydroxamic acid as ZBG to chelate the Zn^{2+} located in HDACs active site, an aromatic moiety, named cap group, which occludes the entrance of the pocket, and a linker connecting the two moieties. Particularly, polycyclic aromatic compounds are quite selective toward HDAC6 (see **2** and **3**), due to its larger substrate binding pocket.[20] As regards the GSK-3β, many inhibitors, for instance **4**–**7**,[21–24] possess a phthalimide-like scaffold, like the aryl-maleimide or the aryl-pyrrolinone, which are acknowledged to competitively bind to the ATP binding site of the enzyme. Bearing in mind these observations, we thought to design a small series of molecules possessing a hydroxamic acid as ZBG and the phthalimide moiety as cap group. In fact, this rather large aromatic moiety might possibly fit in both HDAC1 and HDAC6 and bind the GSK-3β enzyme. The hydroxamic acid has been connected to the ph-

thalimide moiety through polymethylenic linkers of different length (**8**–**11**), with the aid of a thiourea group. The choice of the thiourea group, among several connecting units, was due to its synthetic accessibility.

Synthesis

Detailed descriptions of the synthetic sequences are reported in the Supporting Information (SI).

In Vitro Enzymes Inhibition

Compounds **8**–**11** underwent parallel evaluation for their ability to inhibit GSK-3β, HDAC1, and HDAC6 in comparison to compounds **12** bearing the maleimide moiety responsible for GSK-3β inhibition (see SI for structure), **4**, a known GSK-3β inhibitor, and Vorinostat (**1**), a known HDAC inhibitor. All the new compounds are able to inhibit the activity of the three enzymes in the low micromolar range of concentration. As reported in Table 1, an interesting trend can be defined as compound **11** is more active than compounds **8**–**10** and **12** against GSK-3β. Compound **11** is also the most active inhibitor of HDAC6 of the series with an IC_{50} similar to that of **1** (3.19 ± 0.08 vs 5.6 μM), and the inferior homologues are characterized by lower IC_{50} values (**11** < **9** < **10** < **8**). Conversely, compound **11** is the weakest inhibitor within the series against HDAC1 with the most active of the series being **9** (IC_{50} 2.24 ± 1.17 vs 12.78 ± 0.11 μM of **11**). These effects clearly reflect the importance of the length of the spacers separating the hydroxamic acid and the phthalimide moieties. It is important to note that **1** is not active against GSK-3β, likewise **12** is not active against HDACs.

Table 1

Effects of Compounds 1, 4, and 8–12 on GSK-3β, HDAC1, and HDAC6 Activity

compd	*n*	GSK-3β IC_{50} (μM)[a]	HDAC1 IC_{50} (μM)[a]	HDAC6 IC_{50} (μM)[a]
1		n.a.[b]	0.6 (0.31–3.22)[c,d]	5.6 (5.31–7.45)[c,d]
4		0.05 ± 0.01	n.d.[e]	n.d.[e]
8	1	19.96 ± 1.76	3.75 ± 0.58	18.13 ± 0.17
9	2	9.85 ± 1.00	2.24 ± 1.17	12.58 ± 0.96
10	3	4.11 ± 0.01	5.02 ± 1.2	14.71 ± 0.19
11	4	2.69 ± 0.01	12.78 ± 0.11	3.19 ± 0.08
12		20.22 ± 0.40	n.a.[f]	n.a.[f]

[a]IC_{50} values are defined as the drug concentration that reduces by 50% the target activity and are reported as a mean value of three or more determinations.

[b]n.a.: not active up to 50 μM.

[c]Data from ref (25).

[d]95% confidence interval.

[e]Not determined.

[f]Not active up to 30 μM.

Compound **11** has been selected for a deeper biological investigation due to its high activity against GSK-3β and the two HDAC isoforms. Interestingly, it shows balanced *in vitro* activities against the targets.

Binding Mode Analysis

To gain insights into the mechanism of dual GSK-3β/HDAC inhibition and to elucidate the binding mode of the most active compound **11**, molecular docking calculations were performed using Glide 5.7 in SP mode.[26] As for GSK-3β, an ensemble docking using four representative structures (PDB codes: 1Q3D, 1Q41, 2JLD, 1UV5; see paragraph "X-ray Structures Selection" in SI)[23,27] suggested two possible binding modes. In binding mode A (Figure2a), the maleimide core forms the two typical H-bonds with the hinge region backbone residues V135 and D133, and the thiourea H-bonds, the Q185 backbone carbonyl, and the long aliphatic linker allow the hydroxamic moiety to reach a really polar region of the protein where a deprotonated hydroxamic acid establishes two charge-reinforced H-bonds with the R144 and R141 side chains. On the contrary, in binding mode B (Figure2b), the hydroxamic acid is found under the nucleotide-binding loop. Looking at the **8**–**11** inhibitor profiles in Table 1, it is evident that the shorter the linker, the lower the activity, and only the binding mode A seems to be in accordance with these evidence. As regards the docking of **11** into the HDAC1 and HDAC6 (PDB codes: 4BKX and 5EDU; see SI for choice criteria),[28,29] it converged toward a very similar pose in both isoforms (Figure2c, d, respectively), where the hydroxamic acid coordinates the zinc ion and H-bonds a conserved tyrosine (Y303 in HDAC1, Y782 in HDAC6); the aliphatic spacer is found in the acetyl lysine tunnel stacked between two conserved aromatic side chains (F150 and F205 in HDAC1; F620 and F680 in HDAC6). The thiourea forms a bifurcated H-bond with the side

chains of D99 in HDAC1 and of S538 in HDAC6, the phthalimide contacts a conserved histidine (H28 in HDAC1, H500 in HDAC6) and H-bonds the E98 in HDAC1 and the D497 in HDAC6. Reasonably, the better accommodation of the phthalimide into the larger HDAC6 substrate binding pocket[20] can explain the superior activity of **11** toward HDAC6 with respect to HDAC1.

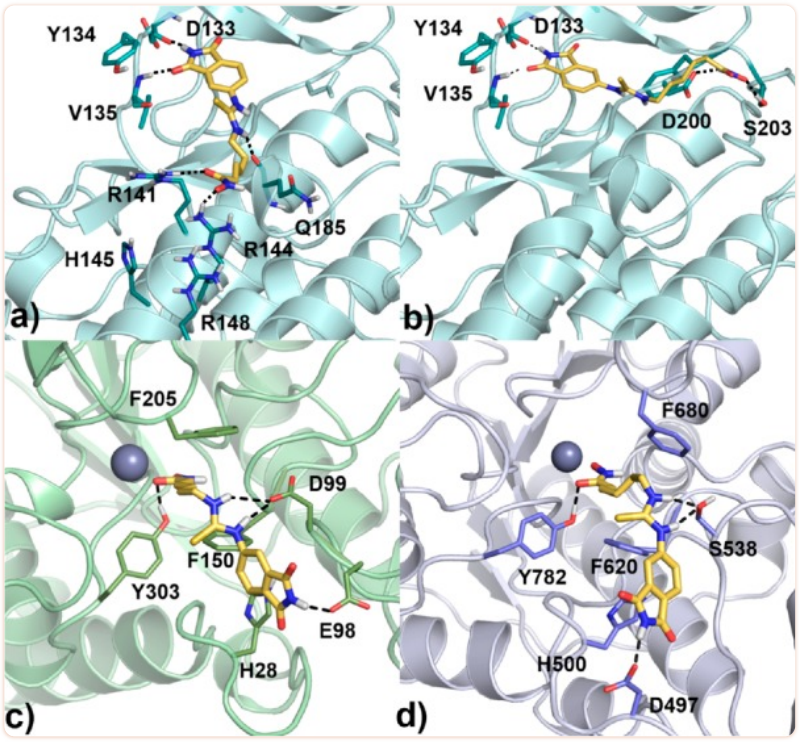

Figure 2

Binding modes A (a) and B (b) of **11** (golden sticks) in the active site of GSK-3β shown as a cyan cartoon and deep teal sticks. Binding poses of **11** into the HDAC1 (c; green cartoon) and HDAC6 (d; violet cartoon) catalytic domains. H-bonds are represented as black dashed lines.

In-Cell Evaluations

In order to evaluate whether the *in vitro* inhibitory activities translate into intracellular inhibition of HDACs, further in-cell-based assays for **11** were carried out. Western blotting analysis was performed using human neuroblastoma SH-SY5Y cell line to determine the effects of compound **11** on the acetylation levels of tubulin and histone H3 at lysines 9/14 (H3K9K14ac) (Figure3a). Cells were treated with compound **11** and its parent compounds, **1** and **12** (5 μM), for 30 h at three different concentrations (0.1, 1.0, and 5.0 μM). Compound **11** was able to induce hyperacetylation of α-tubulin although to a lesser extent than **1**. This effect was already visible at 0.1 μM and was concentration-dependent. However, it was not able to induce similar increase in the acetylation of histone H3, not even at the highest concentration tested. Since tubulin is a substrate of HDAC6 and acetylated tubulin levels function as a biochemical marker for HDAC6 cellular activity, the increase in the level of acetyl-α-tubulin compared to H3K9K14ac could be ascribed to an intrinsic cellular selectivity of compound **11** for HDAC6 isoform. Important effects on tubulin and histone H3 were not observed when cells were treated with **12**.

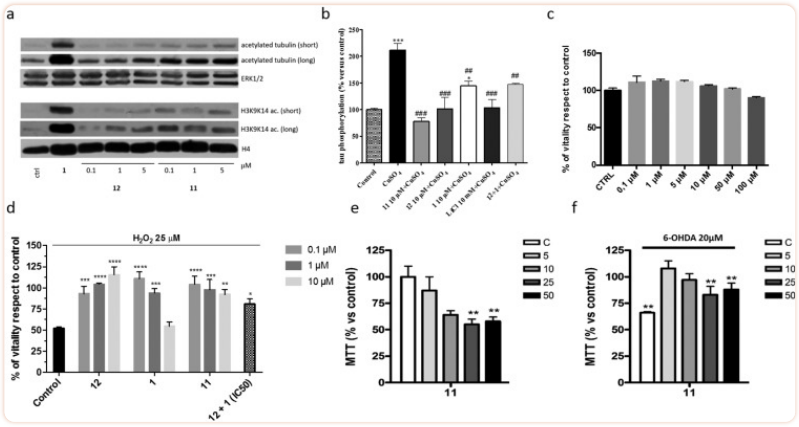

Figure 3

Cell-based assay. (a) Western blot probing for acetylated tubulin and histone H3K9K14ac in the SH-SY5Y cell line after 30 h treatment with **1**, **11**, and **12**. (b) Effects of the compounds on tau phosphorylation. The cells were pretreated with LiCl (10 mM), **1**, **11**, **12** (10 μM), or **1** + **12** for 1 h and then with copper (400 μM) for 16 h. Following incubation time, cells were harvest by scraping, and the pellet was obtained. Subsequently, the extent of tau phosphorylation was determined by immunoenzymatic assay. Absorbance was measured at 450 nm. Values represent the mean ± SEM; $^{*}p < 0.05$, $^{***}p < 0.001$ vs control; $^{\#}p < 0.05$, $^{\#\#}p < 0.01$, $^{\#\#\#}p < 0.001$ vs cells treated with copper. (c) Effect of **11** on SH-SY5Y cell viability after 24 h exposure at 37 °C by MTS assay. Data are expressed as % of vitality respect to control. (d) Effects of **1**, **11**, **12**, and **12** + **1** on SH-SY5Y challenged with H_2O_2. The effect of drugs (0.1–10 μM) on SH-SY5Y cells challenged for 24 h with H_2O_2 (25 and 50 μM) was evaluated by MTS assay. Data are expressed as % of vitality respect to control. $^{*}P < 0.05$, $^{**}P < 0.005$, $^{***}P < 0.001$, vs H_2O_2. (e,f) Neurotoxicity and neuroprotection on 6-OHDA-induced neurotoxicity in primary differentiated CGNs of compound **11**. Results are the mean ± SE of at least 3 different experiments in quadruplicate; $^{**}p < 0.01$, $^{***}p < 0.001$ relative to untreated CGNs; $^{\#\#}p < 0.01$, $^{\#\#\#}p < 0.001$ relative to differentiated CGNs treated with 6-OHDA, Bonferroni's posthoc test following one-way ANOVA.

Then, to assess the effect of compound **11** on tau-hyperphosphorylation, the protein's phosphorylation was induced in differentiated SH-SY5Y cells upon incubation with copper. Copper induced a time-dependent tau phosphorylation in differentiated SH-SY5Y cells, with a peak after 16 h of incubation. Conversely, the level of tau phosphorylation returned to control cell value after 24 h of incubation, probably due to compensatory mechanisms (data not shown). Based on these data, 400 μM copper for 16 h was chosen as experimental conditions. Following, the ability of the compounds to counteract copper-induced tau phosphorylation was examined. LiCl was used as reference control (Figure3b). As reported, compound **11** (10 μM) completely counteracted copper-mediated tau phosphorylation in a major extent compared to LiCl (10 mM), **12**, and **1** (10 μM). Also, the cells were treated with a combination of **1** and **12**, and no significant additive/synergic effect on phospho-tau levels was noticed with respect to single-treated cells (Figure3b). Moreover, the percentage of phospho-tau inhibition was markedly lower with respect to that elicited by the dual-target compound **11**. These data suggest that a dual-target molecule may offer advantages in terms of pharmacokinetics and cellular localization that enable an enhancement of its efficacy.

Since HDAC inhibitors are used in therapy as anticancer drugs, compound **11** was evaluated for its potential toxicity in SH-SY5Y cell line in comparison to compound **1** and **12** using MTS assay (Figure3c and SI). Compound **11** did not show any toxic effects up to 100 μM, while **1** showed a consistent decrease of the cell viability already at 10 μM (see SI). Furthermore, compounds **1**, **11**, and **12** were tested for their ability to counteract oxidative stress-induced neuronal death (Figure3d).

When compounds **1**, **11**, and **12** were administered, the viability was restored to almost the control value expected for **1**. For compound **11**, this effect was evident already at the concentration of 0.1 μM. Cotreatment of **1** + **12**, at their respective IC_{50}s concentration, did not show any synergism in contrasting H_2O_2-induced cell death. Compound **11** turned out to be more efficient than this combination. To further elucidate the activity of compound **11**, the levels of p53 protein were measured after treatments with H_2O_2 in the presence or absence of compound **11** (see SI). Interestingly, in SH-SY5Y cells treated with H_2O_2 (50 μM), p53 expression increases about 30%, and the treatment with compound **11** (10 μM) restored the levels of p53 to control levels. Potential toxic and protective effects of compound **11** were also evaluated on primary differentiated CGNs, and it was found able to completely counteract toxic stimuli induced by 6-hydroxydopamine (6-OHDA) already at 5 μM (Figure3e, f). Again, **11** showed higher activity compared to the combination of **1** + **12** in contrasting 6-OHDA-induced cell death (see SI).

It is well-known that GSK-3β/HDAC inhibition promotes neurogenesis *in vitro* and *in vivo*. To assess whether compound **11** induces neurogenesis in SH-SY5Y cell line, the cells were treated with compound **11** for 24 h, and at the end of the treatment, the mRNA expression of recognized markers of neurogenesis including GAP43, N-myc, and MAP-2 was assessed by RT-PCR analysis. The same experiments were performed by using **1**, **12**, and retinoic acid (RA) as positive control (Figure4a). All the compounds were used at the concentration of 10 μM with the exception of **1**, which was added at the final concentration of 1 μM based on the vitality assay results. All the treatments were able to up-regulate GAP-43 and MAP-2, while N-myc was up-regulated by compound **11**, **1**, and RA but not by compound **12**. Compound **11** increased the expression of MAP-2 and GAP-43 at higher levels than **1**. As expected, RA induced the expression of all the three markers. To confirm the obtained results, the morphology of the differentiated neuronal neurite outgrowth was assessed after cell treatment for 72 h with compounds **11**, **12**, and RA (10 μM) used as positive control. As shown in Figure4b, compound **12** showed a moderate effect in stimulating neurite outgrowth, whereas compound **11** induced a substantial neurite outgrowth comparable to that caused by RA. It was not possible to analyze the effect of **1** due to compound toxicity after 72 h of treatment. Furthermore, we evaluated the ability of compound **1**, **11**, and **12** to modulate the microglial phenotypic switch from the M1 (pro-inflammatory) to the M2 (anti-inflammatory) type thereby decreasing neuroinflammation (Figure5). Indeed, modulation of microglial activation seems to be a valid therapeutic approach in AD and compounds able to modulate the switch from the M1 to M2 phenotype would determine a decrease of neuroinflammation with a parallel increase of neuronal protection and recovery.[30] The immunomodulatory effects of compounds **1**, **11**, and **12** were evaluated on pure primary cultures of microglia by evaluating the expression of NOS2 and MRC1, which are both markers of M1 microglia, or TREM2, marker of M2 microglia. Western blot analysis clearly shows a more evident decrease in both NOS2 and MRC1 expression in cells treated with the compound **11** than in those exposed to **1** and **12**, while TREM2 is unchanged, thus indicating a shift of microglial cells from the M1 neutotoxic to the M2 neuroprotective phenotype and therefore an immunomodulatory activity of compound **11**.

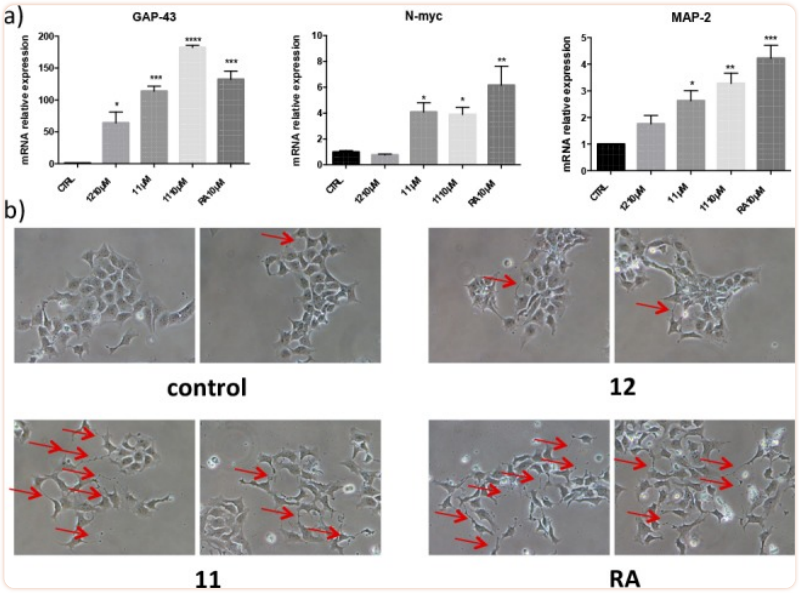

Figure 4

(a) Effect of **11**, **12**, RA (10 μM), and **1** (1 μM) on neurogenesis markers expression (GAP43, N-myc and MAP-2) in SH-SY5Y after 24 h-treatment. The data are expressed as fold of control. (b) Effects of **11**, **12**, and RA (10 μM for 72 h) on neurite outgrowth. Red arrows indicate cells bearing neurites. Pictures were taken at 20× magnification.

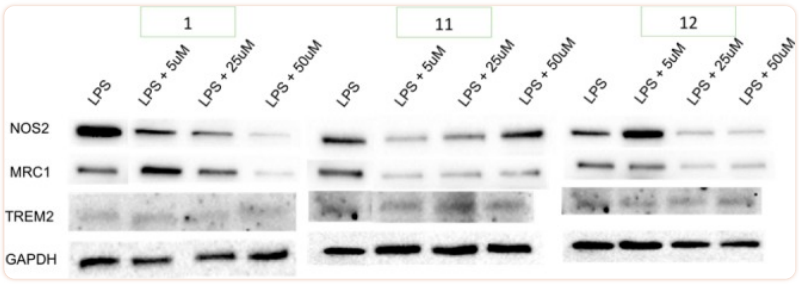

Figure 5

Western blot analysis of NOS2, MRC1, and TREM2 expression in primary microglial cells after a 24 h treatment with LPS in presence or absence of compounds **1**, **11**, and **12**. GAPDH was used as an endogenous control to normalize data.

In Vivo wt-Zebrafish Evaluation

Compound **11** was further profiled for its *in vivo* activity in wild-type zebrafish (*Danio rerio*) (Figure6). Indeed, zebrafish represents an established model system for the *in vivo* validation of GSK-3β inhibitors and assessing drug safety and toxicity. The compounds were added to 5 hpf (50% epiboly), and the embryos were allowed to grow in chemical compound solution up to 2–4 days. Compound **11** showed no lethality in our concentration range (<100 μM). Furthermore, it showed no effects on embryos at the concentration of 25 μM, while at the con-

centration of 50 μM a stunted and crooked tail was observed (Figure6B). This phenotypic effect was more emphasized at 75 μM (Figure6C). At this concentration, some effects on the eyes formation could be observed. The detected effects are consistent with an *in vivo* GSK-3β inhibition.[31] Indeed, the perturbed zebrafish development induced by compound **11** is correlated to the Wnt/β-catenin pathway including GSK-3β. Also, the zebrafish embryo assay provides evidence of exposure and cell penetration of our derivative.

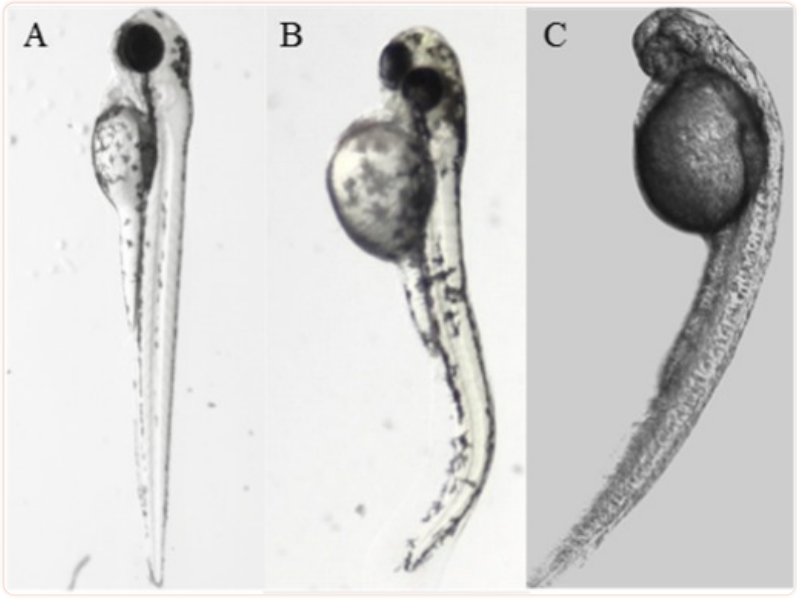

Figure 6

Effects on wild-type zebrafish embryos by compound **11**. (A) Control embryo in 2% DMSO. (B) Embryo treated with **11** at 50 μM. (C) Embryo treated with **11** at 75 μM.

Physicochemical Properties of **11**

One of the main challenges in designing multiple ligands is related to the physical–chemical properties of the designed molecules. Pleasingly, compound **11** is characterized by very good water solubility of 53.76 μg/mL (153.42 μM) and fulfills the requirements of the Lipinski "rule of 5" (see SI).

Conclusions

To sum up, by exploiting a classical design strategy we have obtained the first-in-class small molecule able to exert anti-AD properties by modulating epigenetic and tau-related targets, such as HDAC1, HDAC6, and GSK-3β. Due to its activity profile and thanks to its low MW and high solubility, compound **11** might be considered a promising hit compound to develop an innovative disease-modifying agent. Hit-to-lead optimization studies are currently ongoing and will be reported in due course.

Glossary

ABBREVIATIONS

GAP-43	growth associated protein 43
LPS	lipopolysaccharide
MAP-2	microtubule-associated protein 2
MRC1	mannose receptor Type C1
N-myc	N-myc proto-oncogene protein
NOS2	nitric oxide synthase 2
TREM	triggering receptor expressed on myeloid cells 2

Supporting Information Available

The Supporting Information is available free of charge on the ACS Publications website at DOI: 10.1021/acsmedchemlett.8b00507.

Synthetic procedures, characterization of compounds, biological procedures, and PDB coordinates of described complexes (PDF)

Author Contributions

◆ These authors equally contributed.

Notes

This work was supported by the University of Bologna (RFO), the Italian Ministry for Education, Universities and Research (MIUR), Worldwide Cancer Research (AICR) 15-1002; Bluprint 282510; MIUR20152TE5PK; COSTEPICHEMBIOCM1406; EPIGENMIUR-CNR; and AIRC-17217

Notes

The authors declare no competing financial interest.

Supplementary Material

ml8b00507_si_001.pdf (3.6M, pdf)

References

1. Cummings J. L.; Morstorf T.; Zhong K. Alzheimer's disease drug-development pipeline: few candidates, frequent failures. *Alzheimer's Res. Ther.* 2014, 6, 37. 10.1186/alzrt269. [PMC free article] [PubMed] [CrossRef] [Google Scholar]
2. Mullard A. Pfizer exits neuroscience. *Nat. Rev. Drug Discovery* 2018, 17, 86. 10.1038/nrd.2018.16. [PubMed] [CrossRef] [Google Scholar]
3. Doig A. J.; Del Castillo-Frias M. P.; Berthoumieu O.; Tarus B.; Nasica-Labouze J.; Sterpone F.; Nguyen P. H.; Hooper N. M.; Faller P.; Derreumaux P. Why Is Research on Amyloid-β Failing to Give New Drugs for Alzheimer's Disease?. *ACS Chem. Neurosci.* 2017, 8, 1435–1437. 10.1021/acschemneuro.7b00188. [PubMed] [CrossRef] [Google Scholar]
4. Ramsay R. R.; Popovic-Nikolic M. R.; Nikolic K.; Uliassi E.; Bolognesi M. L. A perspective on multi-target drug discovery and design for complex diseases. *Clin Transl Med.* 2018, 7, 3. 10.1186/s40169-017-0181-2. [PMC free article] [PubMed] [CrossRef] [Google Scholar]
5. Morphy R.; Rankovic Z. Designing multiple ligands - medicinal chemistry strategies and challenges. *Curr. Pharm. Des.* 2009, 15, 587–600. 10.2174/138161209787315594. [PubMed] [CrossRef] [Google Scholar]
6. Decker M.*Design of Hydrid Molecules for Drug Development*. 1 ed.; Elsevier, 2017. [Google Scholar]
7. Oset-Gasque M. J.; Marco-Contelles J. Alzheimer's Disease, the "One-Molecule, One-Target" Paradigm, and the Multitarget Directed Ligand Approach. *ACS Chem. Neurosci.* 2018, 9, 401. 10.1021/acschemneuro.8b00069. [PubMed] [CrossRef] [Google Scholar]
8. Hooper C.; Killick R.; Lovestone S. The GSK3 hypothesis of Alzheimer's disease. *J. Neurochem.* 2008, 104, 1433–9. 10.1111/j.1471-4159.2007.05194.x. [PMC free article] [PubMed] [CrossRef] [Google Scholar]
9. Hwang J. Y.; Aromolaran K. A.; Zukin R. S. The emerging field of epigenetics in neurodegeneration and neuroprotection. *Nat. Rev. Neurosci.* 2017, 18, 347–361. 10.1038/nrn.2017.46. [PMC free article] [PubMed] [CrossRef] [Google Scholar]
10. Fischer A. Targeting histone-modifications in Alzheimer's disease. What is the evidence that this is a promising therapeutic avenue?. *Neuropharmacology* 2014, 80, 95–102. 10.1016/j.neuropharm.2014.01.038. [PubMed] [CrossRef] [Google Scholar]
11. Bardai F. H.; Price V.; Zaayman M.; Wang L.; D'Mello S. R. Histone deacetylase-1 (HDAC1) is a molecular switch between neuronal survival and death. *J. Biol. Chem.* 2012, 287, 35444–53. 10.1074/jbc.M112.394544. [PMC free article] [PubMed] [CrossRef] [Google Scholar]
12. Chen S.; Owens G. C.; Makarenkova H.; Edelman D. B. HDAC6 regulates mitochondrial transport in hippocampal neurons. *PLoS One* 2010, 5, e10848. 10.1371/journal.pone.0010848. [PMC free article] [PubMed] [CrossRef] [Google Scholar]
13. Cook C.; Stankowski J. N.; Carlomagno Y.; Stetler C.; Petrucelli L. Acetylation: a new key to unlock tau's role in neurodegeneration. *Alzheimer's Res. Ther.* 2014, 6, 29. 10.1186/alzrt259. [PMC free article] [PubMed] [CrossRef] [Google Scholar]

14. Wang G.; Shi Y.; Jiang X.; Leak R. K.; Hu X.; Wu Y.; Pu H.; Li W. W.; Tang B.; Wang Y.; Gao Y.; Zheng P.; Bennett M. V.; Chen J. HDAC inhibition prevents white matter injury by modulating microglia/macrophage polarization through the GSK3β/PTEN/Akt axis. *Proc. Natl. Acad. Sci. U. S. A.* 2015, 112, 2853–8. 10.1073/pnas.1501441112. [PMC free article] [PubMed] [CrossRef] [Google Scholar]

15. Leng Y.; Liang M. H.; Ren M.; Marinova Z.; Leeds P.; Chuang D. M. Synergistic neuroprotective effects of lithium and valproic acid or other histone deacetylase inhibitors in neurons: roles of glycogen synthase kinase-3 inhibition. *J. Neurosci.* 2008, 28, 2576–88. 10.1523/JNEUROSCI.5467-07.2008. [PMC free article] [PubMed] [CrossRef] [Google Scholar]

16. Sharma S.; Taliyan R. Synergistic effects of GSK-3β and HDAC inhibitors in intracerebroventricular streptozotocin-induced cognitive deficits in rats. *Naunyn-Schmiedeberg's Arch. Pharmacol.* 2015, 388, 337–49. 10.1007/s00210-014-1081-2. [PubMed] [CrossRef] [Google Scholar]

17. Lehár J.; Krueger A. S.; Avery W.; Heilbut A. M.; Johansen L. M.; Price E. R.; Rickles R. J.; Short G. F.; Staunton J. E.; Jin X.; Lee M. S.; Zimmermann G. R.; Borisy A. A. Synergistic drug combinations tend to improve therapeutically relevant selectivity. *Nat. Biotechnol.* 2009, 27, 659–66. 10.1038/nbt.1549. [PMC free article] [PubMed] [CrossRef] [Google Scholar]

18. Cuadrado-Tejedor M.; García-Osta A.; Ricobaraza A.; Oyarzabal J.; Franco R. Defining the mechanism of action of 4-phenylbutyrate to develop a small-molecule-based therapy for Alzheimer's disease. *Curr. Med. Chem.* 2011, 18, 5545–5553. 10.2174/092986711798347315. [PubMed] [CrossRef] [Google Scholar]

19. Butler K. V.; Kalin J.; Brochier C.; Vistoli G.; Langley B.; Kozikowski A. P. Rational design and simple chemistry yield a superior, neuroprotective HDAC6 inhibitor, tubastatin A. *J. Am. Chem. Soc.* 2010, 132, 10842–10846. 10.1021/ja102758v. [PMC free article] [PubMed] [CrossRef] [Google Scholar]

20. **a.** Santo L.; Hideshima T.; Kung A. L.; Tseng J. C.; Tamang D.; Yang M.; Jarpe M.; van Duzer J. H.; Mazitschek R.; Ogier W. C.; Cirstea D.; Rodig S.; Eda H.; Scullen T.; Canavese M.; Bradner J.; Anderson K. C.; Jones S. S.; Raje N. Preclinical activity, pharmacodynamic, and pharmacokinetic properties of a selective HDAC6 inhibitor, ACY-1215, in combination with bortezomib in multiple myeloma. *Blood* 2012, 119, 2579–89. 10.1182/blood-2011-10-387365. [PMC free article] [PubMed] [CrossRef] [Google Scholar]
b. Yang E. G.; Mustafa N.; Tan E. C.; Poulsen A.; Ramanujulu P. M.; Chng W. J.; Yen J. J.; Dymock B. W. Design and Synthesis of Janus Kinase 2 (JAK2) and Histone Deacetlyase (HDAC) Bispecific Inhibitors Based on Pacritinib and Evidence of Dual Pathway Inhibition in Hematological Cell Lines. *J. Med. Chem.* 2016, 59, 8233–8262. 10.1021/acs.jmedchem.6b00157. [PubMed] [CrossRef] [Google Scholar]

21. Coghlan M. P.; Culbert A. A.; Cross D. A.; Corcoran S. L.; Yates J. W.; Pearce N. J.; Rausch O. L.; Murphy G. J.; Carter P. S.; Roxbee Cox L.; Mills D.; Brown M. J.; Haigh D.; Ward R. W.; Smith D. G.; Murray K. J.; Reith A. D.; Holder J. C. Selective small molecule inhibitors of glycogen synthase kinase-3 modulate glycogen metabolism and gene transcription. *Chem. Biol.* 2000, 7, 793–803. 10.1016/S1074-5521(00)00025-9. [PubMed] [CrossRef] [Google Scholar]

22. La Pietra V.; La Regina G.; Coluccia A.; Famiglini V.; Pelliccia S.; Plotkin B.; Eldar-Finkelman H.; Brancale A.; Ballatore C.; Crowe A.; Brunden K. R.; Marinelli L.; Novellino E.; Silvestri R. Design, synthesis, and biological evaluation of 1-phenylpyrazolo[3,4-e]pyrrolo[3,4-g]indolizine-4,6(1H,5H)-diones as new glycogen synthase kinase-3β inhibitors. *J. Med. Chem.* 2013, 56, 10066–78. 10.1021/jm401466v. [PubMed] [CrossRef] [Google Scholar]

23. Bertrand J. A.; Thieffine S.; Vulpetti A.; Cristiani C.; Valsasina B.; Knapp S.; Kalisz H. M.; Flocco M. Structural characterization of the GSK-3beta active site using selective and non-selective ATP-mimetic inhibitors. *J. Mol. Biol.* 2003, 333, 393–407. 10.1016/j.jmb.2003.08.031. [PubMed] [CrossRef] [Google Scholar]

24. Zou H.; Zhou L.; Li Y.; Cui Y.; Zhong H.; Pan Z.; Yang Z.; Quan J. Benzo[e]isoindole-1,3-diones as potential inhibitors of glycogen synthase kinase-3 (GSK-3). Synthesis, kinase inhibitory activity, zebrafish phenotype, and modeling of binding mode. *J. Med. Chem.* 2010, 53, 994–1003. 10.1021/jm9013373. [PubMed] [CrossRef] [Google Scholar]

25. Giacomini E.; Nebbioso A.; Ciotta A.; Ianni C.; Falchi F.; Roberti M.; Tolomeo M.; Grimaudo S.; Cristina A. D.; Pipitone R. M.; Altucci L.; Recanatini M. Novel antiproliferative chimeric compounds with marked histone deacetylase inhibitory activity. *ACS Med. Chem. Lett.* 2014, 5, 973–8. 10.1021/ml5000959. [PMC free article] [PubMed] [CrossRef] [Google Scholar]

26. *Schrödinger Release 2011–4 Glide*; Schrödinger LLC: New York, 2011. [Google Scholar]

27. Atilla-Gokcumen G. E.; Pagano N.; Streu C.; Maksimoska J.; Filippakopoulos P.; Knapp S.; Meggers E. Extremely tight binding of a ruthenium complex to glycogen synthase kinase 3. *ChemBioChem* 2008, 9, 2933–6. 10.1002/cbic.200800489. [PMC free article] [PubMed] [CrossRef] [Google Scholar]

28. Millard C. J.; Watson P. J.; Celardo I.; Gordiyenko Y.; Cowley S. M.; Robinson C. V.; Fairall L.; Schwabe J. W. Class I HDACs share a common mechanism of regulation by inositol phosphates. *Mol. Cell* 2013, 51, 57–67. 10.1016/j.molcel.2013.05.020. [PMC free article] [PubMed] [CrossRef] [Google Scholar]

29. Hai Y.; Christianson D. W. Histone deacetylase 6 structure and molecular basis of catalysis and inhibition. *Nat. Chem. Biol.* 2016, 12, 741–7. 10.1038/nchembio.2134. [PMC free article] [PubMed] [CrossRef] [Google Scholar]

30. Peña-Altamira E.; Prati F.; Massenzio F.; Virgili M.; Contestabile A.; Bolognesi M. L.; Monti B. Changing paradigm to target microglia in neurodegenerative diseases: from anti-inflammatory strategy to active immunomodulation. *Expert Opin. Ther. Targets* 2016, 20, 627–40. 10.1517/14728222.2016.1121237. [PubMed] [CrossRef] [Google Scholar]

31. Nishiya N.; Oku Y.; Kumagai Y.; Sato Y.; Yamaguchi E.; Sasaki A.; Shoji M.; Ohnishi Y.; Okamoto H.; Uehara Y. A zebrafish chemical suppressor screening identifies small molecule inhibitors of the Wnt/β-catenin pathway. *Chem. Biol.* 2014, 21, 530–540. 10.1016/j.chembiol.2014.02.015. [PubMed] [CrossRef] [Google Scholar]